CHEMICAL ENGINEERING TRANSACTIONS
VOL. 109, 2024
A publication of AIDIC
The Italian Association of Chemical Engineering
Online at www.cetjournal.it
Guest Editors: Leonardo Tognotti, Rubens Maciel Filho, Viatcheslav Kafarov

ISBN 979-12-81206-09-0; **ISSN** 2283-9216
DOI: 10.3303/CET24109045

The Conversion of 5-Chloromethylfurfural into 5-Methoxymethylfurfural via Nucleophilic Substitution: Kinetic Modeling

Gianfranco Giorgianni[a,*], Rober-Jan van Putten[b], Jan C. Van der Waal[c], Siglinda Perathoner[a], Gabriele Centi[a], Salvatore Abate[a]

[a] Dept. ChiBioFarAm - Chimica Industriale, University of Messina and ERIC Aisbl, Viale F. Stagno D'Alcontres 31, Messina 98166, Italy
[b] Avantium, Zekeringstraat 29, 1014 BV Amsterdam, The Netherlands
[c] TNO Netherlands Organization of Applied Scientific Research, Leeghwaterstraat 44, 2628 CA, Delft, the Netherlands
gianfranco.giorgiorgianni@unical.it

The nucleophilic substitution of chlorine into the 5-chloromethylfurfural (CMF) by methanol is a high potential route for the production of 5-methoxymethylfurfural (MMF), allowing the production of 2,5-furandicarboxylic acid, an important intermediate for polyester synthesis with larger yield and selectivity than 5-hydroxymethylfurfural. However, HCl, produced during the nucleophilic substitution, leads to the formation of by-products like humins or methyl levulinate, and it is faced by adding bases to the reaction with the side effect of producing large amounts of waste as salts. On the contrary, optimizing the MMF yields in the absence of any base could allow the recycling of the produced HCl into the CMF production process, with benefits for the whole route. To optimize the reaction, CMF was reacted with methanol at low concentration, using a multi-reactor in batch mode, to maximize the MMF yield at 10, 20, 40, and 50 °C. Finally, a lumped kinetic model was employed to analyse the reaction further. The yield of MMF and its corresponding acetal increase with a reaction time and temperature of up to 60 % in 1.5 h.

1. Introduction

The drive for a more sustainable society has led to a boost in bio-based chemistry research. Research has recently shifted from mono, disaccharide (glucose, fructose, sucrose), and pure polysaccharides (starch, cellulose) feedstocks to the cruder lignocellulosic biomass. From an economic point of view, it is of interest to efficiently convert crude feedstock in as few steps as possible to products that can be readily purified, especially in the case of potential bulk chemicals. Therefore, a wealth of research has been dedicated to the conversion of carbohydrates to furanics, like furfural, 2-methylfuran (Giorgianni et al., 2023), and especially 5-hydroxymethylfurfural (HMF, Scheme 1a) (van Putten et al., 2013).
HMF is a high-potential bio-based building block (Munoz De Diego et al., 2011; Werpy & Petersen, 2004). It can readily oxidize to 2,5-furandicarboxylic acid (FDCA, Scheme 1.1b), a key polyester and polyamide production monomer. However, efficiently yielding HMF from sugars or other crude feedstocks remains challenging, often requiring complex solvent systems (ionic liquids, aprotic polar solvents) (van Putten et al., 2013). A novel approach involves using 5-chloromethylfurfural (CMF) as an intermediate (Scheme 1.1e-f), a hydrophobic HMF analog, more amenable to isolation and obtainable from cellulosic biomass using a hydrochloric acid biphasic system (Scheme 1.1c) (Breeden et al., 2013; Mascal & Nikitin, 2009).
CMF's susceptibility toward nucleophilic substitution reactions in water or alcohol prompts its conversion to various compounds, including HMF and 5-alkoxymethylfurfurals (Scheme 1.1d-e) (Mascal & Nikitin, 2008). These reactions release hydrochloric acid, which in water leads to by-products like levulinic acid (LA) and formic acid (FA) (Scheme 1.1d) (Girisuta et al., 2006). However, performing the CMF nucleophilic substitution in the presence of alcohol (Scheme 1.1e), and low amounts of water could minimize the formation of levulinics. Additionally, etherification leads to increased stability and, especially for methanol (MeOH) and ethanol, a lower

Paper Received: 16 December 2023; Revised: 16 February 2024; Accepted: 25 March 2024
Please cite this article as: Giorgianni G., Van Putten R.-J., Van Der Waal J.C., Perathoner S., Centi G., Abate S., 2024, The Conversion of 5-chloromethylfurfural Into 5-methoxymethylfurfural via Nucleophilic Substitution: Kinetic Modelling, Chemical Engineering Transactions, 109, 265-270 DOI:10.3303/CET24109045

boiling point than for HMF, favouring storage and work-up/purification of RMFs. The conversion of CMF in MeOH, used as a reactant and solvent, proceeds through the series of reactions represented in Scheme 1.2. Apart from the expected nucleophilic substitution on the chloromethyl group, leading to MMF (Scheme 1.2a), with subsequent elimination of HCl, both the presence of MeOH and HCl leads to the formation of acetals of CMF (CMFA, Scheme 1.2d) and MMF (MMFA Scheme 1.2b-c) due to the presence of the aldehydic group (Teixeira et al., 2020). In addition, in the presence of HCl, CMF and other intermediates can also be converted into methyl levulinate (LM) and methyl formate (FM) (Scheme 1.2e) (Onkarappa & Dutta, 2019) and other by-products, such as humins by condensation reactions of furfural derivatives (Scheme 1.2f). Although by-product formation can be limited by using organic or inorganic bases, it also produces salts, while recycling the produced HCl back into the CMF synthesis step could benefit the process's sustainability and profitability.

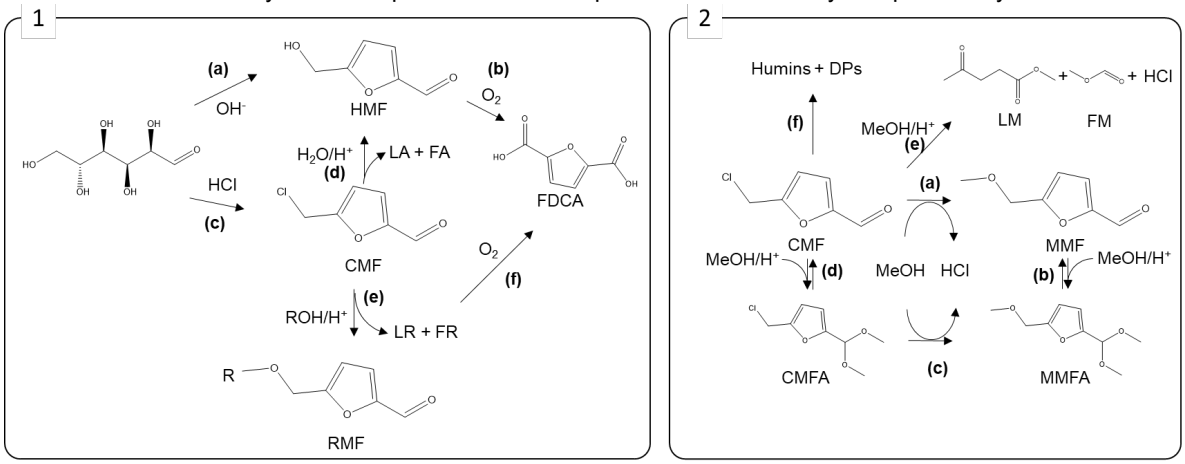

Scheme 1 – (1) Routes to FDCA thorough HMF and CMF, and (2) simplified CMF conversion pathways in MeOH

Therefore, here, the reaction of CMF in anhydrous MeOH will be studied at different temperatures and without a base to maximize the MMF yields. This should lead to a better understanding of the conversion of CMF into RMF and get a feel for its industrial application.

2. Methods

2.1 Chemicals and Materials

Purified 5-(chloromethyl)furfural (CMF), the reaction substrate, was generously provided by Micromidas Inc. Analytical grade 2-(chloromethyl)-5-(dimethoxymethyl)furan (CMFA), levulinic acid (LA), methyl levulinate (LM), 5-methoxymethylfurfural (MMF), 2-(Dimethoxymethyl)-5-(methoxymethyl)furan (MMFA), 1,4-dioxane, acetonitrile, saccharine, anhydrous methanol (MeOH), and ultrapure water were purchased from Sigma Aldrich (Merck) and used without further purification.

2.2 Kinetic Experiments

All the kinetic experiments were performed by using a Crystal16 multi-reactor (Technobis Crystallization Systems, previously known as Avantium Crystallization Systems), equipped with 16 glass vial batch reactors of 1 mL each, separately into four parallel temperature blocks, capable of working between -20 and 140 °C.
In our experiments, each vial reactor was (1) filled with 0.500 ± 0.05 mL, closed and (2) placed within each reactor block, precooled or preheated at 10, 20, 30, and 50°C, and stirred at 700 rpm. Then, (3) the reaction was started by adding a weighted amount of CMF into each reactor vial ($2.350 – 3.100 \cdot 10^{-3}$ g), to reach an initial concentration of 0.0355 mol/L (CMF_0). The batch reaction time varied between 0.25 and 4 h. (4) The reaction was ended by quenching the reactor vials into an ice bath. Finally, (5) the resulting solutions were quickly filtered, diluted with the analysis solvents (including external standards), and analyzed by gas chromatography (GC) and Ultra-performance liquid chromatography (UPLC).

2.3 Analytical Methods

CMF, CMFA, LA, and LM were analysed using a Trace 1310 GC (Thermo Scientific) equipped with an FID detector and an HP DB-624 column (30 m x 0.25 m x 1.4 µm, J&W Agilent), using 1,4-dioxane and acetonitrile as external standard and analysis solvent, respectively. The GC was operated at 250°C, with a 2.5 mL/min He flow. MMF and MMFA were measured by an Acquity UPLC (Waters), equipped with an Acquity ULPC BEH C18

(2.1x5.0 mm, 1.7 µm, Waters) column, and employing saccharine and ultrapure water as external standard and analysis solvent, respectively. The employed mobile phase (0.6 mL/min), consisting of acetonitrile/methanol (1:1, A) and water (0.2 wt% TFA, B) was delivered with a gradient starting from 98% A (2% B) up to 2% A (98% B). MMF and saccharine were detected on a PDA detector at 230 and 250 nm, respectively.

2.4 Reaction Performance Evaluation

Humins are challenging to measure due to their insolubility in most solvents. Therefore, these species and other by-products were calculated by difference with the molar balance, according to Eq(1). The conversion of CMF and product yields were estimated through Eq(2-3).

$$c_{UM} = c_{CMF_0} - (c_{CMF} + c_{CMFA} + c_{MMF} + c_{MMFA}) \quad (1)$$

$$\varepsilon_{CMF} = \frac{c_{CMF} - c_{CMF_0}}{c_{CMF_0}} \quad (2)$$

$$Y_i = \frac{c_i}{c_{CMF_0}} \quad (3)$$

All the above-reported c_i terms are concentrations of products and intermediates expressed in mol/L.

2.5 Kinetic Modelling

The synthesis of MMF from CMF in MeOH presents a complex kinetic network involving, apart from nucleophilic substitutions, acetalization reactions, and ring opening reactions, involving several intermediates (Scheme 1.2). Therefore, a rigorous mechanistic approach would require a very extensive set of results. Here, with the primary purpose of describing the nucleophilic substitution of CMF. Thus, to achieve this purpose, acetalization reactions were excluded from the model, assuming the same kinetics in the nucleophilic substitution of CMF and CMFA, leading to MMF and MMFA, respectively. Therefore, a simplified lumped kinetic model was developed for describing the reactions (see Scheme 2), with CMF and MMF and their respective acetals considered in the CMF_s and MMF_s lumps, respectively, as in Eq(4-5). This assumption is also justified because acetalization reactions can be easily reversed. Therefore, it is possible to consider the sum of MMF and MMFA as a key product in practice.

$$c_{CMF_s} = c_{CMF} + c_{\mathrm{CMFA}} \quad (4)$$

$$c_{MMF_s} = c_{MMF} + c_{\mathrm{MMFA}} \quad (5)$$

ML and MF were supposed to be formed exclusively by acid-catalyzed decomposition of CFM_s as this lump presents the higher concentration at the beginning of the reaction, assuming for simplicity a first-order kinetics on the concentration of CMF_s and H^+, similar to what has been observed for HMF in water (Girisuta et al., 2006). The unmeasured products were considered in the same lump (UM) and assumed to consist of Humins (Onkarappa & Dutta, 2019), which, for simplicity, were assumed as derived from the condensation of CMF_s, which is the most reactive substrate, considering a first-order reaction with respect to CMF_s. Also, a kinetic model considering the effect of H^+ was considered, resulting in a slightly less good fitting (not reported). The kinetic equations describing the model are reported in Eq(5-11) along with their respective initial conditions. The Arrhenius expressions for k_1, k_2, and k_3 were re-parameterized by Eq(12-14) at 30°C (T_{ave}).

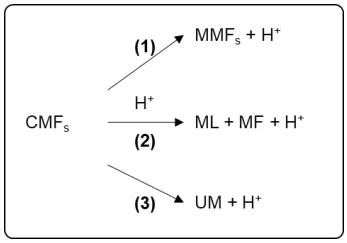

Scheme 2 – Lumped kinetic network

$$\frac{d\,[\mathrm{CMF_s}]}{dt} = -\mathrm{k_1}[\mathrm{CMF_s}] - \mathrm{k_2}\,[\mathrm{CMF}_s]\,[\mathrm{H^+}] - \mathrm{k_3}[\mathrm{CMF_s}] \quad (5)$$

$$\frac{d\,[\mathrm{MMF_s}]}{dt} = \mathrm{k_1}[\mathrm{CMF_s}] \tag{6}$$

$$\frac{d\,[ML]}{dt} = \frac{d\,[\mathrm{MF}]}{dt} = \mathrm{k_2}[\mathrm{CMF_s}][\mathrm{H^+}] \tag{7}$$

$$\frac{d\,[\mathrm{UM}]}{dt} = \mathrm{k_3} \cdot [\mathrm{CMF_s}] \tag{8}$$

$$\frac{d\,[\mathrm{H^+}]}{dt} = \mathrm{k_1}[\mathrm{CMF_s}] + \mathrm{k_2}\,[\mathrm{CMF_s}][\mathrm{H^+}] + \mathrm{k_3} \cdot [\mathrm{CMF_s}] \tag{9}$$

$$[\mathrm{CMF_s}]_0 = [\mathrm{CMF_0}] \tag{10}$$

$$[\mathrm{MMF_s}]_0 = [\mathrm{ML}]_0 = [FM]_0 = [\mathrm{H^+}]_0 = [Hu]_0 = 0 \tag{11}$$

$$k_1 = k_{1,T_{ave}} \cdot e^{-\frac{E_1}{R}\cdot\left(\frac{1}{T}-\frac{1}{T_{ave}}\right)} \tag{12}$$

$$k_2 = k_{2,T_{ave}} \cdot e^{-\frac{E_2}{R}\cdot\left(\frac{1}{T}-\frac{1}{T_{ave}}\right)} \tag{13}$$

$$k_3 = k_{3,T_{ave}} \cdot e^{-\frac{E_3}{R}\cdot\left(\frac{1}{T}-\frac{1}{T_{ave}}\right)} \tag{14}$$

The above-reported ODEs set was solved by parametric numerical integration using Wolfram Mathematica 12, the LSODA method (Wolfram Research Inc., 2014), and the initial CMF (CMF0) concentrations for each reaction batch. All the parameters were fitted by using the whole experimental dataset at once for all the tested temperatures and all the initial conditions (global fitting) by nonlinear regression, using the "NMinimize" optimization algorithm and assuming the same weight for all the experimental data. Only CMF_s, MMF_s, and LM experimental data were used for the fitting procedure without considering the calculated concentration of UM.

3. Results and Discussion

3.1 Main Reaction Performance

The main results, in terms of CMF conversion, CMFA, MMF, MMFA, and LM yields, are reported in Figure 1 at all the tested temperatures. The CMF conversion in each batch increased over time, with the testing temperature, and it was complete in all the cases after 4 h.

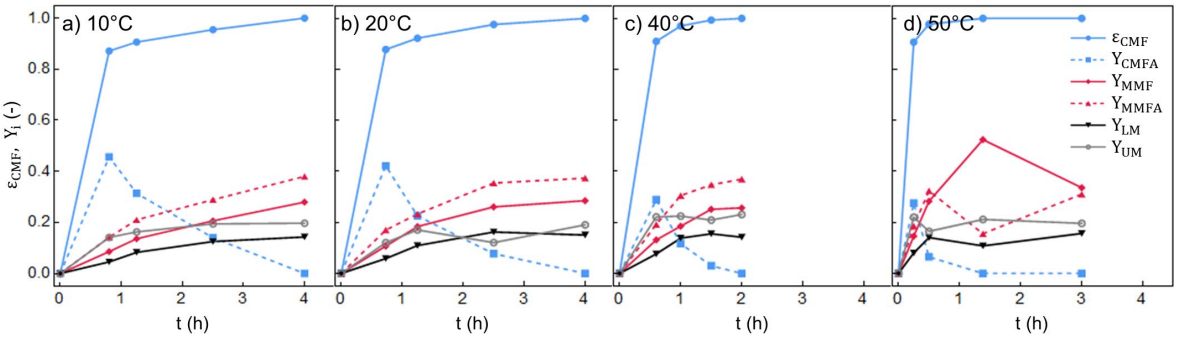

Figure 1 – CMF conversion (ε_{CMF}) and product yields (Y_i) at a) 10, b) 20, c) 40, and d) 50 °C (each point in time represent a different batch, with an average initial CMF_0 conc. Of 0.035 mol/L)

The CMFA yield, consistent with the kinetic Scheme 1b, passed through a maximum with respect to time at all the tested temperatures and achieved the highest value at 10°C (Y_{CMFA}, 0.45). All other products increased with respect to time. After 2 h of reaction, MMFA and MMF were the most abundant products. Among these, at 10 – 40°C, the MMFA yield was always larger than MMF. Conversely, at 50°C, the MMF yield was comparable to or larger than MMFA. The MMF yield, our main target product, after 4h, was comparable at all the tested

temperatures (Y_{MMF}, 0.31). Interestingly, the highest MMF yield was, apparently, achieved at 50°C, after 1.4 h (Y_{MMF}, 0.51), consistent with a corresponding decrease in the MMFA yield (Y_{MMFA}: 0.15). Also, LM was maximized in all the cases after 4 h. Notice that the yield of unmeasured products increased over time with a similar trend at all the measured temperatures. The observed Y_{UM} trends, and the lack of marked maxima, are compatible with the formation of insoluble Humins, even though, considering the acetalization chemistry, some hemiacetals of CMF and MMF might be included in this product fraction. A kinetic model was developed to understand the trends better and explore the reaction's performance, and the simulated reaction performance was discussed.

3.2 Kinetic Results

Due to the important simplifying assumptions it is based on, it is important to remark that the proposed kinetic model is not meant to represent the true kinetics of the reaction but to help in describing the reaction trends within the experimental window it was fitted in. Although presenting important simplifying assumptions, the proposed model describes well the experimental lumped concentrations of CMF_s, LM, and MMF_s at all the tested temperatures (Figure 2b-c), with acceptable residuals, as shown in the parity plot reported in (Figure 2e). Moreover, the model takes very well into account the variations in the initial concentrations of CMF (CMF(0)) in each batch (see Figure 2a-d. Accordingly, the fitted parameters present p-values well below the accepting criteria and present narrow confidence intervals (Table 1).

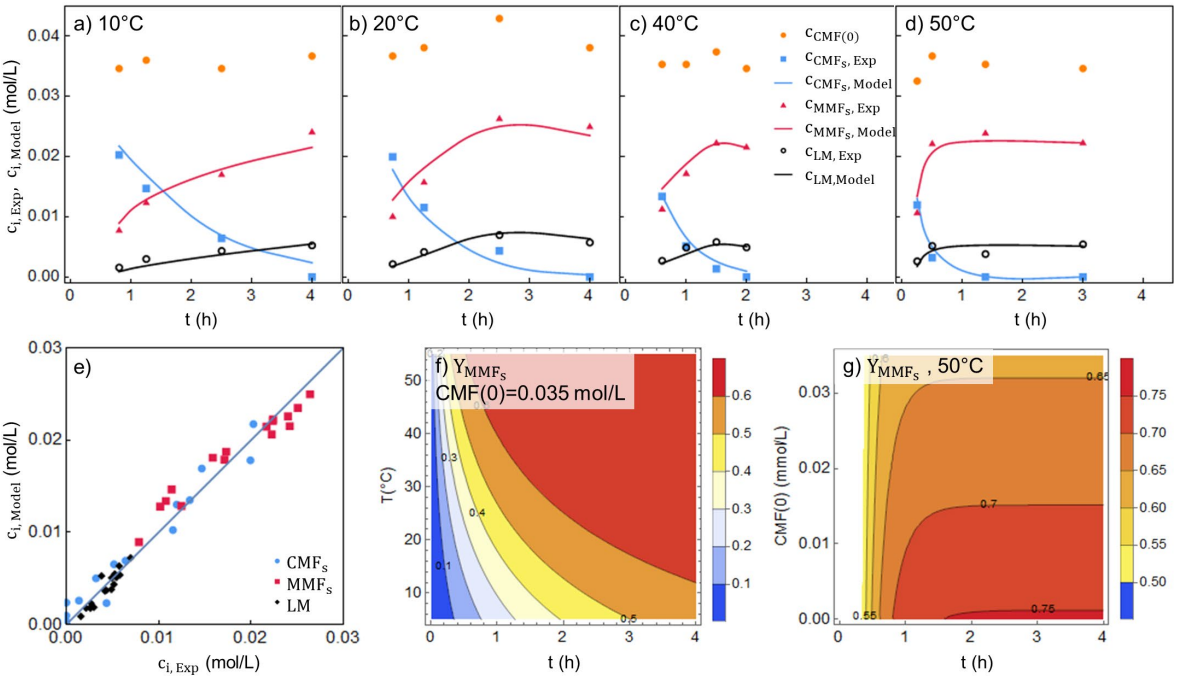

Figure 2 – Lumped model fitting at a) 10, b) 20, c) 40, and d) 50°C, e) MMF_s yields model predicted at CMF(0) = 0.035 mol/L with respect to temperature and time, and g) at 50°C with respect to time and the initial CMF concentration (the lumped concentrations reported in the plots are calculated as: CMF_s = CMF + CMFA; MMF_s = MMF + MMFA; in a-d, the connecting lines, represent only an interpolation of the model result points at the corresponding time and it was reported only for better visualization)

The kinetic constant for the production of MMF_s ($k_1(T_{ave})$), in agreement with the experimental data, is three times larger than the one leading to unmeasured products ($k_3(T_{ave})$), while the large value of the kinetic constant leading to LM ($k_2(T_{ave})$) agrees with the large dependence of the reaction on the H^+ concentration. However, contrary to the expectations, all the fitted activation energies are quite similar to each other. Therefore, the simplifying assumptions of the model do not allow differentiating the nucleophilic substitution's activation energy. On the contrary, the good fitting results still allow exploring the reaction's performance within the investigated experimental window, which, industrially speaking, could allow important economic conclusions on the reaction. Accordingly, we focused on the MMF_s lump yield resulting from the calculated model to maximize its yield. The model results indicate an increase in the MMF_s yield with increasing the reaction time and temperature (Figure 2f), even though, in the explored experimental window, it does not overcome 60 % (Y_{MMFs} = 0.6). Moreover, it

is quite apparent that by increasing the temperature from 10 to 50°C, it is possible to reduce the reaction time from more than 5 h to 1.5 h to get a MMF_s yield of 0.6. According to the model results, at 50°C, a further increase in the MMF_s yield, from 0.6 to 0.65, could be achieved by decreasing the initial CMF concentration (Figure 2g) from 0.035 to 0.02 mol/L, even though considering the already low CMF(0), this could make to process much less productive for a modest increase in the MMF_s yield.

Table 1 – Estimated parameters

Parameters	Estimated ± 95%	P-values
$k_1(T_{ave})$ [h^{-1}]	1.059 ± 0.073	$1.7037 \cdot 10^{-29}$
$k_2(T_{ave})$ [$h^{-1} \cdot mol^{-1} \cdot L$]	15.6 ± 2.8	$6.1236 \cdot 10^{-14}$
$k_3(T_{ave})$ [h^{-1}]	0.352 ± 0.074	$4.77886 \cdot 10^{-12}$
E_1 [$kJ \cdot mol^{-1}$]	34.6 ± 3.5	$5.89249 \cdot 10^{-23}$
E_2 [$kJ \cdot mol^{-1}$]	32.4 ± 9.9	$6.10353 \cdot 10^{-8}$
E_3 [$kJ \cdot mol^{-1}$]	33.8 ± 10.9	$1.97807 \cdot 10^{-7}$
R^2	0.988419	
Adj R^2	0.986765	
Estimated variance	$2.14132 \cdot 10^{-6}$	

4. Conclusions

This study provides valuable insights into optimizing the conversion of CMF to MMF, a critical process for the sustainable production of valuable intermediates in polyester synthesis. Using a simplified kinetic model, we effectively described the reaction trends and identified conditions for maximizing MMF yield. By the employed kinetic model, we found that increasing the temperature reduced the reaction time while maintaining high yields. Moreover, operating without a base potentially contributes to the process's sustainability by reducing waste salts and potentially allowing recycling produced hydrochloric acid. Future research will explore further process optimizations and industrial scalability.

References

Breeden, S. W., Clark, J. H., Farmer, T. J., Macquarrie, D. J., Meimoun, J. S., Nonne, Y., & Reid, J. E. S. J. 2013. Microwave heating for rapid conversion of sugars and polysaccharides to 5-chloromethyl furfural. Green Chem., 15(1), 72–75. 10.1039/C2GC36290B

Giorgianni, G., Perathoner, S., Centi, G., Soo-Tang, S.-H., de Jong, E., van der Waal, J. C., & Abate, S. 2023. Exploring the hydrogenation of furfural in the liquid phase by high-throughput screening of commercial catalysts: Effects of temperature, solvents, and promoters on the production of 2-methylfuran. Chemical Engineering Research and Design, 197, 968–983. 10.1016/j.cherd.2023.08.010

Girisuta, B., Janssen, L. P. B. M., & Heeres, H. J. 2006. A kinetic study on the decomposition of 5-hydroxymethylfurfural into levulinic acid. Green Chemistry, 8(8), 701. 10.1039/b518176c

Mascal, M., & Nikitin, E. B. 2008. Direct, high-yield conversion of cellulose into biofuel. Angewandte Chemie - International Edition, 47(41), 7924–7926. 10.1002/anie.200801594

Mascal, M., & Nikitin, E. B. 2009. Dramatic advancements in the saccharide to 5-(chloromethyl)furfural conversion reaction. ChemSusChem, 2(9), 859–861. 10.1002/cssc.200900136

Munoz De Diego, C., Schammel, W., Dam, M. A., & Gruter, G. J. M. 2011. Method for the preparation of 2,5-furandicarboxylic acid and esters thereof (Patent No. PCT/NL2010/050653, WO2011043660). https://patentscope.wipo.int/search/en/detail.jsf?docId=WO2011043660

Onkarappa, S. B., & Dutta, S. 2019. High-Yielding Synthesis of 5-(alkoxymethyl)furfurals from Biomass-Derived 5-(halomethyl)furfural (X=Cl, Br). ChemistrySelect, 4(19), 5540–5543. 10.1002/slct.201900279

Teixeira, M. G., Natalino, R., & da Silva, M. J. 2020. A kinetic study of heteropolyacid-catalyzed furfural acetalization with methanol at room temperature via ultraviolet spectroscopy. Catalysis Today, 344, 143–149. 10.1016/j.cattod.2018.11.071

van Putten, R.-J., van der Waal, J. C., de Jong, E., Rasrendra, C. B., Heeres, H. J., & de Vries, J. G. 2013. Hydroxymethylfurfural, A Versatile Platform Chemical Made from Renewable Resources. Chemical Reviews, 113(3), 1499–1597. 10.1021/cr300182k

Werpy, T., & Petersen, G. 2004. Top Value Added Chemicals from Biomass: Volume I -- Results of Screening for Potential Candidates from Sugars and Synthesis Gas. 10.2172/15008859

Wolfram Research Inc. 2014. Mathematica 10.0 (10.0). Wolfram Research, Inc. https://www.wolfram.com